


Cite this: *RSC Adv.*, 2021, **11**, 1376

Received 11th September 2020  
Accepted 7th December 2020

DOI: 10.1039/d0ra07807g

[rsc.li/rsc-advances](http://rsc.li/rsc-advances)

## Recent developments in the nanomaterial-catalyzed green synthesis of structurally diverse 1,4-dihydropyridines

Ritu Mathur,<sup>a</sup> Khushal Singh Negi,<sup>b</sup> Rahul Shrivastava <sup>b</sup> and Rashmy Nair <sup>\*c</sup>

1,4-Dihydropyridine (1,4-DHP), a privileged heterocyclic scaffold, has been extensively utilized in various biological and therapeutic applications. In this review article, we discussed the role of different nano-catalysts, nanoflakes, nanocomposites, and other green-supported nanomaterials in the synthesis of a biologically active and vital pharmaceutical precursor 1,4-DHP and its derivatives such as polyhydroquinoline, benzopyranopyridines, and dihydropyridine since 2015. It is evident that although the use of various tailored nanostructures under different conditions to optimize the synthesis of 1,4-DHP and its compounds has provided sustainable and efficient proposals, yet the development of greener practices in the synthesis of 1,4-DHPs, which can be applied to design new synthetic routes and sequences in process development, is a far-reaching task to be accomplished.

### Introduction

The increased awareness on the environment and climate-related issues has encouraged organic chemists to develop eco-compatible chemical processes incorporating the basic principles of green chemistry such as atom economy, non-toxic reactants, use of benign solvent, and efficient catalyst. Among the different aspects of a green chemical process, the utilization of an effective non-toxic catalyst has played a pivotal role in the designing of green and sustainable chemical transformations

owing to the capability of the catalyst to reduce the temperature, pressure, and reagent-based waste along with the enhancement of the selectivity of a reaction, which potentially circumvents unwanted side reactions.<sup>1</sup> Catalysis through nanomaterials has been proven to be an attractive approach to frame greener chemical pathways, based on their unique features such as a larger reactive surface to volume ratio with higher sensitivity and selectivity, milder reaction conditions, and possibility of recycling and reusing the catalyst. It has been observed that nanomaterials have collective merits of both heterogeneous and homogeneous catalytic systems. Higher surface area allows facile contact between reactants, making the nano-catalyst behave like a homogeneous catalyst, whereas being insoluble in the reaction mixture, it acts similar to a heterogeneous

<sup>a</sup>Department of Chemistry, Zakir Husain Delhi College, New Delhi-110002, India

<sup>b</sup>Department of Chemistry, Manipal University Jaipur, Jaipur 303007, Rajasthan, India

<sup>c</sup>Department of Chemistry, S. S. Jain Subodh P. G. (Autonomous) College, Jaipur 302004, Rajasthan, India. E-mail: rashmy\_xyz@live.com


Dr. Ritu Mathur is Assistant Professor of Chemistry at Zakir Husain Delhi College, University of Delhi, New Delhi, India. Dr Ritu did her Master's in Chemistry from the Department of Chemistry, University of Rajasthan, Jaipur, India. She received her doctoral degree in the year 2004 from the University of Rajasthan, Jaipur, India. Her research interests include areas of synthetic organic chemistry, materials science, and studies on nanoparticles.



Mr. Khushal Singh Negi did his Master's in Organic Chemistry from Vidya Bhawan Rural Institute Udaipur, Rajasthan, 2007 and Bachelor's in Education from Mantram Teacher Training College, Udaipur, Rajasthan, 2008. Presently, he is pursuing PhD from Manipal University Jaipur, Rajasthan. His research interest includes the synthesis of heterocyclic moieties with beneficial biological activities.



catalyst. The insolubility of the nanomaterial facilitates its easy separation from the reaction mixture, thus allowing it to be acceptable for green chemical manufacturing processes at the industrial level.<sup>2-4</sup> Also, nanomaterial-catalyzed chemical processes offer fast and selective chemical reactions with exceptionally high product yields along with the ease of catalyst recoverability and reusability. The detailed literature assessment revealed that over the last decade, various nanomaterials have been used as catalysts in various structural transformations with several advantages over conventional catalysts. The different types of nanomaterials such as metal oxide nanoparticles, solid-supported metal oxide nanoparticles, functionalized and non-functionalized carbon nanomaterials, mesoporous silica nanomaterials, silica-supported nanomaterials, magnetic nanoparticles/functionalized magnetic nanoparticles, and nano-zeolites have been exclusively used for the synthesis of different heterocyclic scaffolds. These nanomaterials have their specific advantages, for example, metal oxide/mixed-metal oxide nanoparticles are reusable and cost effective, with tuneable surfaces that provide high selectivity and excellent yields of the target product. Carbon nanomaterials have exceptional physical properties such as high oxidation stability, good chemical inertness, high surface area, and unusual electron conductivity, making them competent catalyst for environmentally benign synthetic processes for a variety of organic conversions. Silica nanoparticles or mesoporous silica materials due to their uniform pores, high mechanical and chemical stability, and large surface area are widely used nanoscale support materials in designing nanocatalysts. Magnetic nanoparticles or magnetic nano-supports offer the advantages of easy separation from the reaction mixture to avoid the loss of valuable catalyst, thereby improving the purity and yield of the product and minimizing the operational cost of the methodology.

To design and develop efficient novel drug molecules, a range of heterocyclic building blocks have been explored based on their ability to cease the inherent toxicity of numerous pathogens.<sup>5,6</sup> Among various heterocyclic ring systems, 1,4-dihydropyridine (1,4-DHP) and its derivatives serve as

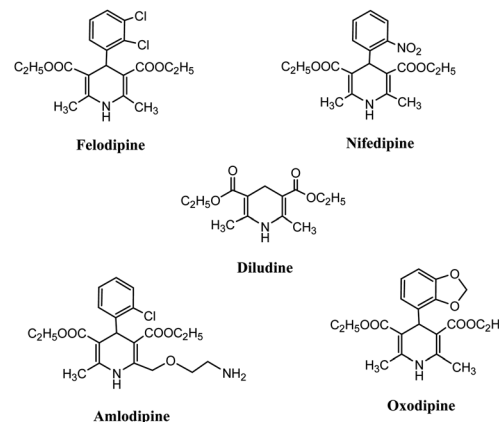


Fig. 1 1,4-Dihydropyridine moiety-containing commercial drugs.

important heterocyclic scaffolds that have gained special attention among synthetic chemists due to their special features, such as distinctive molecular structure, low molecular mass, and widespread pharmaceutical activities. The 1,4-dihydropyridine core is extensively utilized in several biological and therapeutic applications such as anti-tumor,<sup>7</sup> calcium blocker agents in heart disease, antianginal,<sup>8</sup> antihypertensive,<sup>9</sup> antidiabetic,<sup>10</sup> and antimicrobial<sup>11</sup> agents. The importance of the 1,4-DHP nuclei is evident from the fact that it is prevalent in several commercial drugs such as Felodipine, Diludine, Amlodipine, Oxodipine, and Nifedipine, as shown in Fig. 1. In addition, it is also known for its reducing properties<sup>12</sup> and as an active intermediate<sup>13</sup> in important organic transformations. Its optically active moiety works as a valid precursor in the synthesis of different chiral N-heterocycles.<sup>14</sup>

Conventionally, 1,4-dihydropyridine (1,4-DHP) and its derivatives could be synthesized *via* the well-known Hantzsch reaction through the one-pot multicomponent synthesis comprising of cyclo-condensation amongst two molecules of  $\beta$ -ketoester, aldehyde, and ammonia in EtOH under refluxing condition, as depicted in Scheme 1.<sup>15</sup>

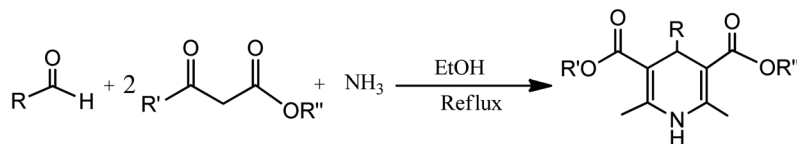


Dr. Rahul Srivastava is Associate Professor of Organic Chemistry at the Manipal University Jaipur, Jaipur, India. Dr Srivastava received his Master's degree from Indian Institute of Technology, Delhi in 2002. He obtained his PhD degree from Indian Institute of Technology Delhi, India in 2009. His research interest includes molecular recognition, calixarene- and cyclotrimeratrylenene-based receptor molecules, nanosensors, chemosensors, nano-catalysts, and multicomponent reactions.



Dr. Rashmy Nair is Associate Professor of Organic Chemistry at S. S. Jain Subodh P. G. (Autonomous) College, Jaipur, Rajasthan, India. Dr Nair completed her Master's degree from the Department of Chemistry, University of Rajasthan, Jaipur in the year 1999. She received her doctoral degree in the year 2004 from the University of Rajasthan, Jaipur, India. Her areas of research interests include synthetic methodology, nanocatalysis, multicomponent reactions, and materials science.





Scheme 1 Classical single pot multicomponent reaction-Hantzsch synthesis.

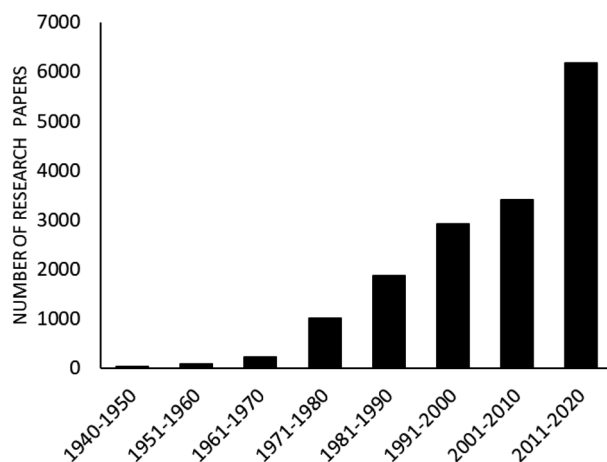


Fig. 2 Progress in research papers on the synthesis of 1,4-dihydropyridine (1,4-DHP) and its derivatives. Data collected from search hits on Scifinder and Google scholar using key words: 1,4-dihydropyridines, Hantzsch reaction, nanomaterials catalyzed synthesis of 1,4-DHPs etc.

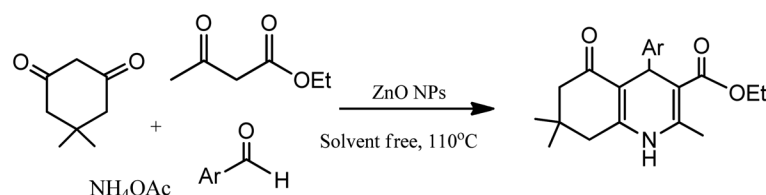
The advantages of Hantzsch reaction such as its facetiousness and tolerance of a wide range of substrates makes it a frequently-employed approach for 1,4-DHP synthesis. Despite several advantages of this conventional synthetic route, various research groups have offered different improvements so as to avoid limitations such as corrosive acid usage, low to moderate yields, toxic solvents, high temperatures, and long reaction times, which are associated with this methodology.<sup>16,17</sup> In this context, a number of homogeneous, heterogeneous, and various kinds of nanomaterials are utilized as catalysts to overcome the drawbacks associated with Hantzsch reaction so as to synthesize pharmacologically important 1,4-dihydropyridine motifs. It is found that interest in the synthesis of 1,4-DHPs containing molecules *via* eco-compatible and environmentally conscious chemical processes using different nanomaterials has continuously increased, which can be adjudged by Fig. 2. As depicted in the figure, ample research papers

published since 2010 are based on various green chemical processes using different magnetic and non-magnetic nanomaterials as catalysts in the synthesis of 1,4-DHPs-containing derivatives.

The focus of this article is largely on exploring the applications of various nanomaterials that have been used so far for the three/four component synthesis of 1,4-DHP derivatives *via* the single-pot multicomponent pathway. The reported reviews<sup>18-20</sup> on nanomaterial-catalyzed heterocyclic ring systems synthesis either discussed only one or two types of nanomaterials or emphasized on the synthesis of several diverse heterocyclic compounds rather than considering one heterocyclic moiety. The examples described here are grouped under sections such as non-magnetic nanoparticles and magnetic nanoparticle-catalyzed synthesis of 1,4-DHPs and its derivatives with detailed discussion on the synthesis and advantages of the chemical transformation thereof. The brief synthesis and characterization of some novel nanomaterials are discussed in this review. The details pertaining to other nanomaterials are adequately presented in the cited papers. We as synthetic chemists have focused in a full-fledged manner on the synthetic aspects of 1,4-DHP and its related derivatives through multicomponent reactions, nanomaterials, and novel green methodologies in an environmentally benign way.

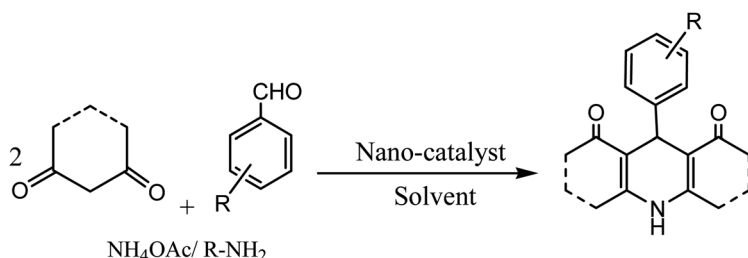
## Non-magnetic metal oxide/mixed-metal oxide nanoparticles catalyzed synthesis of 1,4-DHP

The development of renewable and cheap, non-magnetic nanocatalysts has always been a core area of research as they provide excellent yields, ease of catalyst recovery, and product purification from the reaction medium. In this perspective, metal oxides and mixed-metal oxide nanoparticles, either alone or on a solid support, have contributed significantly in various organic transformations because of the tuneable characteristics of their versatile surfaces.<sup>21</sup> Zinc oxide nanoparticles are widely used as catalyst in various organic transformations as compared



Scheme 2 Zinc oxide nanoparticle-assisted Hantzsch condensation under solventless condition to produce 1,4-DHPs and its derivatives.



Table 1 Non-magnetic metal oxide/mixed-metal oxide nanoparticle-catalyzed protocol for the synthesis of 1,4-DHP-containing scaffolds<sup>a</sup>

Entry	Catalyst	Temperature (°C)	Solvent	Time (min)	Yield <sup>b</sup> (%)	Ref.
1	ZnO NPs	110	Solvent free	40	61–94	23
2	ZnO NPs	80	Solvent free	80–135	92	24
3	Cu doped ZnO NPs	80	Water	Reflux	90	27
4	ZnO@SnO <sub>2</sub> NPs	80	Solvent free	17	96	28
5	CuO nanoflakes	70	EtOH (30):H <sub>2</sub> O (70)	140	80–90	29
6	TiCl <sub>2</sub> /nano-γ-Al <sub>2</sub> O <sub>3</sub>	90	Solvent free	90	90	30
7	NaMgBi <sub>0.85</sub> Eu <sub>0.15</sub> WO <sub>6</sub>	Room temperature	EtOH	120	95	31
8	ZrP <sub>2</sub> O <sub>7</sub>	Reflux	EtOH	45	85	34
9	NiO-ZrO <sub>2</sub>	Room temperature	EtOH	20–45	89–98	35
10	CuI/SMI (polystyrene- <i>co</i> -maleic anhydride)	80	Solvent free	30	81–93	36

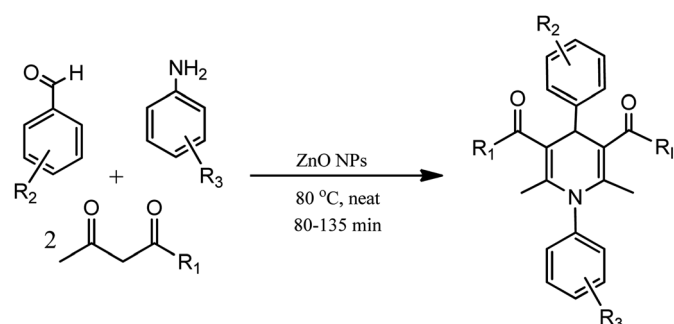
<sup>a</sup> Reaction conditions: aldehyde (1.0 mmol), ethyl acetoacetate (1.0 mmol), NH<sub>4</sub>OAc (1.5 mmol), dimedone (1.0 mmol). <sup>b</sup> Isolated yields.

to other metal oxides due to its unique features such as environment friendliness and inexpensiveness.<sup>22</sup> Zinc oxide nanoparticles are also used as heterogeneous Lewis acid catalyst for solvent-free Hantzsch condensation using substituted aldehydes, dimedone, NH<sub>4</sub>OAc, and ethyl acetoacetate to produce excellent yields of polyhydroquinoline and 1,4-dihydropyridine derivatives, as depicted in Scheme 2 (Table 1; entry 1). The reaction conditions for the optimization illustrated that the reaction was carried out with higher efficiency at 110 °C temperature and with 0.01 g of the catalyst. The excellent yields, shorter time of reaction, solvent-free conditions, simple work-up procedure, and no formation of side products are some merits of this method.<sup>23</sup>

In an alternative method, *N*-substituted derivatives of 1,4-dihydropyridine were prepared in high yields by taking substituted anilines along with 15 mol% zinc oxide nanoparticles at 80 °C under neat conditions, as shown in Scheme 3 (Table 1; entry 2). It was found that when different substituted aldehydes and anilines with either electron releasing and/or electron withdrawing groups were used, the *para*-substituted compounds gave better yields due to less steric effect in comparison to *meta*-substituted ones. The easy recoverability and reusability of the catalyst, short reaction times, neat reaction condition, excellent yields, and easy work up procedure are some of the advantages of this synthetic process.<sup>24</sup>

The properties of zinc oxide nanoparticles can be modified by doping with other metals so as to meet some specific applications. Copper acts as an important doping metal due to its similar chemical and physical properties as that of zinc oxide and the ability of copper to alter the luminescence and micro-structure of these zinc oxide crystals.<sup>25,26</sup> Therefore, copper-doped zinc oxide nanocrystalline powder was synthesized and

used as a catalyst for 1,4-DHPs' synthesis in water at 100 °C (Table 1; entry 3). The high product yields, easy work-up procedure, simple catalyst preparation, and use of water as a solvent are the noteworthy advantages of this developed protocol. The optimization studies suggested that the usage of 10 mol% catalyst gave excellent yields. It was found that electron-withdrawing substituents on benzaldehyde enhanced the reaction rate to afford higher yields of the desired product, whereas it was opposite in the case of electron-releasing substituents.<sup>27</sup> In another attempt, ZnO@SnO<sub>2</sub> nanoparticles were explored as a catalyst for the synthesis of 1,4-dihydropyridine derivatives due to their significant properties such as non-toxicity, strong oxidizing power, reusability, high activity, and long-term stability. The synthesis of 1,4-dihydropyridines was attempted by condensing NH<sub>4</sub>OAc, substituted aldehydes, and ethyl acetoacetate with 10 mol% ZnO@SnO<sub>2</sub> at 80 °C under neat conditions (Table 1; entry 4). During optimization, it was found



Scheme 3 Zinc oxide nanoparticle-catalyzed synthesis of *N*-substituted derivatives of 1,4-dihydropyridine under neat conditions.



Scheme 4 Neutral  $\text{NaMgBi}_{0.85}\text{Eu}_{0.15}\text{WO}_6$  nanoflake-catalyzed preparation of 1,4-dihydropyridines in EtOH solvent.

that the catalytic activity of the reported catalyst was superior to other metal oxide nanoparticles such as  $\text{ZnO}$ ,  $\text{SnO}_2$ , and  $\text{Fe}_3\text{O}_4$  tested for reaction under similar conditions. The electronic studies revealed that aromatic aldehydes bearing electron withdrawing substituents exhibited higher product yields in a shorter time. Also, excellent yields, minimum catalyst loading, cleaner reaction profile, recyclability of the catalyst, and lesser reaction times are some other attractive aspects of this protocol.<sup>28</sup>

Other metal oxide or mixed-metal oxide nanoparticles are also utilized as the catalyst in Hantzsch condensation reaction, for example, the condensation of ethyl/methyl acetoacetate,  $\text{NH}_4\text{OAc}$ , and aromatic aldehyde was carried out to synthesize 1,4-DHP derivatives in good yields using cost-effective copper oxide nanoflakes in EtOH–water mixture (30 : 70) at 70 °C under microwave conditions (Table 1; entry 5). The nanoflake-assisted synthesis offered several advantages such as the use of green solvent, simple synthetic methodology, mild reaction conditions, cheap catalyst, and easy workup procedure. In addition, recycled copper oxide nanoflakes were reused for the next three cycles and maintained the same activity.<sup>29</sup>

The catalytic activity of  $\text{TiCl}_2$ /nano- $\gamma$ - $\text{Al}_2\text{O}_3$  nanoparticles was explored through the synthesis of 1,4-dihydropyridine derivatives *via* the solvent-free multicomponent coupling reaction of aldehyde, 1,3-dicarbonyl compounds, and  $\text{NH}_4\text{OAc}$ , which gave excellent yields in shorter times (Table 1; entry 6). During the evaluation of the catalytic activity taking different solvents and exploring various heating methods, the best yield of the reaction was found to be acquired in neat conditions at 90 °C after 90 min.<sup>30</sup>

A mixture of ethyl acetoacetate, benzaldehyde, ammonia derivative, and nanoflakes of  $\text{NaMgBi}_{0.85}\text{Eu}_{0.15}\text{WO}_6$  were stirred at room temperature for 2.0 h, affording pure dihydropyridines in magnificent yields, as shown in Scheme 4 (Table 1; entry 7). The optimization studies revealed that the aromatic aldehydes with electron attracting groups decreased the yields, whereas electron-releasing groups gave good yields in short times. The high yield of the products can be attributed to the inherent photocatalytic nature of the catalyst. Some prominent advantages of this synthesis are the green process, shorter time of reaction, high yields, easy product isolation, and environment-friendly catalyst, which is reusable without a considerable loss of activity.<sup>31</sup>

Zirconium pyrophosphate nanoparticles are neutral, mild, and environmentally benign catalysts, and their remarkable performance in terms of the selectivity, reactivity, and high temperature stability have encouraged scientists to explore them for the synthesis of 1,4-dihydropyridines.<sup>32,33</sup> A three-

component mixture of ethyl acetoacetate, aldehyde,  $\text{NH}_4\text{OAc}$ , and  $\text{ZrP}_2\text{O}_7$  nanoparticles was refluxed in EtOH to afford 1,4-dihydropyridines (Table 1; entry 8). The detailed investigation studies revealed that the best results were obtained using 10% mmol nanoparticles.<sup>34</sup>

A four-component single-pot strategy was employed using aromatic, heteroaromatic, and aliphatic aldehydes for synthesizing twelve novel 1,4-dihydropyridine derivatives in high yields by introducing  $\text{NiO}$ -loaded zirconia ( $\text{NiO}/\text{ZrO}_2$ ), an efficient, economical, and expedient catalyst (Table 1; entry 9). The optimization conditions exhibited that the yield of the product was maximized by using the reported catalyst in EtOH at 25 °C within 20 to 45 min. On the basis of these results, various  $\text{ZrO}_2$ -based mixed oxide catalysts, namely,  $\text{CuO}/\text{ZrO}_2$ ,  $\text{CeO}_2/\text{ZrO}_2$ , and  $\text{NiO}/\text{ZrO}_2$ , were investigated. 2.5%  $\text{NiO}/\text{ZrO}_2$  gave an impressive yield of 98% in a short time of 20 min, whereas 2.5%  $\text{CuO}/\text{ZrO}_2$  gave 73% yield in 60 min and 2.5%  $\text{CeO}_2/\text{ZrO}_2$  gave 81% yield in 45 min. The authors concluded that 2.5 wt% of  $\text{NiO}/\text{ZrO}_2$  gave better catalytic activity, which is attributed to the availability of higher amount of active  $\text{NiO}$  sites in the blend with  $\text{ZrO}_2$  as well as the active material being evenly distributed on the support's surface, which combine to selectively speed up the reaction rate.<sup>35</sup>

$\text{CuI}$  nanoparticles immobilized on SMI (polystyrene-*co*-maleic anhydride) act as an effective catalyst for the facile and efficient green synthesis of substituted 1,4-dihydropyridine derivatives under solvent free conditions, as presented in Scheme 5 (Table 1; entry 10). Computational studies on the catalytic activity of  $\text{CuI}/\text{SMI}$  demonstrated that the reaction was accelerated due to interaction between the carbonyl group and the  $\text{CuI}$  nanoparticles. Wide scope, short reaction times, simple operation and work up procedures, high yield, and catalyst recyclability for five consecutive runs without any substantial loss in the catalytic activity are some merits of this method.<sup>36</sup> In addition, Tabassum *et al.* have reported the  $\text{CuI}$ -catalyzed

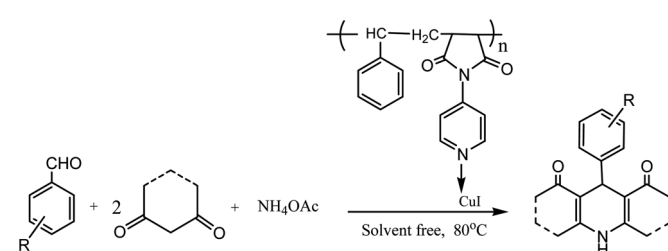
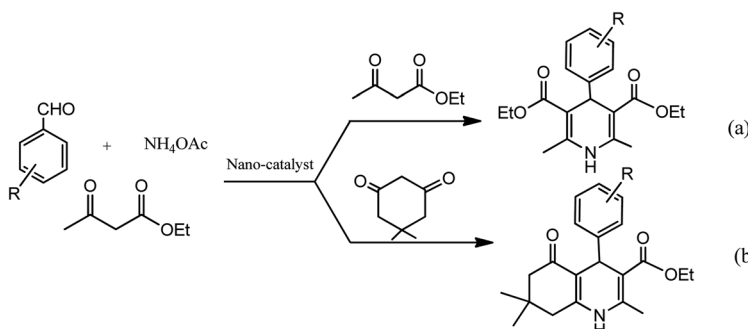
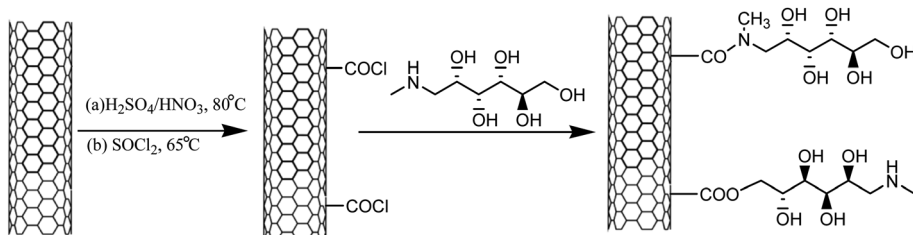
Scheme 5 Multicomponent synthesis of 1,4-DHP derivatives using  $\text{CuI}$  immobilized on SMI (polystyrene-*co*-maleic anhydride) under neat conditions.

Table 2 Functionalized carbon nanomaterial as a nano-catalyst/support for the synthesis of 1,4-DHP and its derivatives<sup>a</sup>

Entry	Catalyst	Temperature (°C)/Ultrasonic probe (W)	Solvent	Time (min)	Yield <sup>b</sup> (%)	Ref.
1	Aminated MWCNT	80	EtOH	180	96	43
2	Ultrasound CNT@meglumine	70	EtOH	15	(a) 82–95 (b) 85–94	44
3	PdRuNi@GO NPs	70	DMF	45	88–93	45

<sup>a</sup> Reaction conditions: arylaldehyde (1.0 mmol), NH<sub>4</sub>OAc (1.0 mmol), ethyl acetoacetate (2.0 mmol), dimedone (1.0 mmol). <sup>b</sup> Isolated yields.



Scheme 6 Synthesis of MWCNTs@meglumine.

multicomponent synthetic reaction for dihydropyridines using ultrasound wave irradiation.<sup>37</sup>

### Functionalized carbon nanomaterial as the nanocatalyst/support for the synthesis of 1,4-DHPs

The excellent selectivity, reusability and easy workup procedure of solid-supported nanomaterials prompted organic chemists to utilize these nanomaterials as catalysts in various organic transformations.<sup>38</sup> Carbon nanomaterials, due to their extraordinary physical properties such as good chemical inertness, high oxidation stability, high surface area, and exceptional electron conductivity,<sup>39</sup> have been widely used as solid supports in diverse forms such as graphene, fibres, and helices in different dimensions for various catalysts.<sup>40–42</sup> An amino-functionalized multiwalled carbon nanotube as the solid base catalyst was reported to prepare 1,4-dihydropyridines (Table 2; entry 1). A mixture of arylaldehyde derivative, ethyl acetoacetate and NH<sub>4</sub>OAc (or dimedone, arylaldehyde derivative, ethyl acetoacetate, NH<sub>4</sub>OAc), and aminated carbon nanotubes as the catalyst in EtOH were refluxed at 80 °C to get the product in high yields. The synthesized products were screened for their

antimicrobial activities against a dozen microorganisms and some fungi strains. Some derivatives were found to be effective against both Gram-positive bacteria and fungi.<sup>43</sup>

In view of the recent surge in the development of green protocols for synthesis, an effective, inexpensive, solid, mild, highly efficient, and reusable heterogeneous catalyst, MWCNTs@meglumine, was developed *via* a three-step process, wherein the immobilization of meglumine was done on the carbon nanotube surface to yield MWCNTs@meglumine, as shown in Scheme 6.

The optimization studies revealed that the loading of 10 mol% MWCNTs@meglumine was found to be sufficient to catalyze the reaction in EtOH at room temperature conditions under an ultrasonic probe of 70 W to afford excellent yield of the corresponding products (Table 2; entry 2). Clean and green reaction conditions, shorter reaction times, high product yield, heterogeneity, and catalyst reusability are some of the main advantages of the reported method.<sup>44</sup>

Further, graphene oxide-supported PdRuNi@GO nanomaterial was synthesized and characterized by TEM, HRTEM, XRD, and XPS techniques. The TEM image of the synthesized



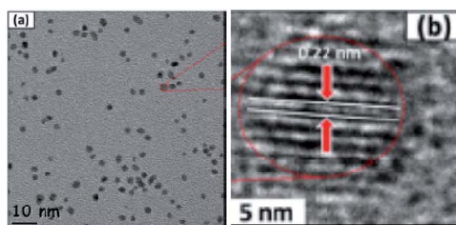


Fig. 3 (a) TEM and (b) HR-TEM images of the synthesized PdRuNi@GO nanoparticles. Adapted with permission from ref. 45. Copyright Royal Society of Chemistry.

PdRuNi@GO showed that the particles are distributed on the support of graphene oxide, as shown in Fig. 3.

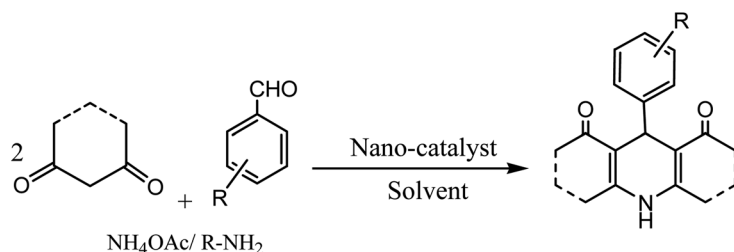
The prepared PdRuNi@GO NPs were employed as a catalyst for the synthesis of 1,4-DHP *via* the one-pot multicomponent reaction of different aldehydes with ethyl acetoacetate, NH<sub>4</sub>OAc, and dimedone at 70 °C in dimethyl formamide. (Table 2; entry 3). The authors exhibited that the outstanding catalytic activity of PdRuNi@GO NPs is mainly due to the high percentage of metal contents, low crystalline particle size, and high monodispersity. The high product yields, shortest reaction time, exceptional catalytic activity, and mild conditions are some of the advantages of the method. In addition, it was found that the recovered catalyst was successfully used for five successive runs without losing its catalytic activity and there was no considerable change in the metal (Pd, Ru, Ni) content.<sup>45</sup>

## Functionalized silica nanoparticles/support-catalyzed synthesis of 1,4-DHPs

Mesoporous silica materials have unique properties such as a large surface area, uniform pore size, and high mechanical/thermal/chemical stability, and are therefore widely used as catalysts in organic transformations because the ordered

mesoporous network of these materials allows the free diffusion of products and reactants.<sup>46–48</sup> The acidic nature of silica-supported SnCl<sub>4</sub> prompted various acid catalyzed organic conversions<sup>49</sup> and helped in avoiding the disadvantages associated with homogeneous SnCl<sub>4</sub> such as handling, storage problems, and toxicity. The SnCl<sub>4</sub>@SiO<sub>2</sub> nanoparticle-catalyzed synthesis of 1,4-dihydropyridines was carried out through the four-component condensation reaction in EtOH under sonication conditions (Table 3; entry 1). Simple work-up, high yields, shorter reaction time, and reusability are some evident benefits of this protocol. The detailed optimization studies exhibited that EtOH was the best solvent under ultrasonic irradiation at 20 Hz and 40 W to obtain a pure crystalline product in higher yield and shorter time with lower catalyst loading. Along with these, it was observed that the SnCl<sub>4</sub>@SiO<sub>2</sub> NPs were easily recoverable and reusable for four consecutive cycles, retaining the same activity.<sup>50</sup> In the process for the development of an eco-friendly approach for the synthesis of polyhydroquinolines and 1,4-dihydropyridines derivatives,  $\beta$ -cyclodextrin imidazolium-based cationic ionic liquid supported on silica was used as a green and reusable heterogeneous catalyst (Table 3; entry 2).  $[\beta\text{CD/Im}](\text{OTs})_2$ @silica was prepared through a three-step procedure. Initially, mono-Ts- $\beta$ CD was prepared by the reaction of  $\beta$ CD with TsCl. Mono-Ts- $\beta$ CD was then reacted with 1,4-bis(imidazol-1-yl)-butane to give  $[\beta\text{CD/Im}](\text{OTs})_2$ .  $[\beta\text{CD/Im}](\text{OTs})_2$ @silica was synthesized by the reaction of  $[\beta\text{CD/Im}](\text{OTs})_2$  with 3-chloropropyl-trimethoxysilane, followed by tetraethoxysilane. After taking the model reaction into consideration, the superiority of the reported catalyst was demonstrated over the other catalysts. It was detected that the  $[\beta\text{CD/Im}](\text{OTs})_2$ @silica catalyst required the shortest reaction time and lowest catalyst loading to yield the desired products in high yield, proving it to be the best choice for the reaction. It was also established that the catalyst could be potentially reused up to four times without a reduction in the catalytic activity. Some of the unique advantages of this catalytic method are the mild

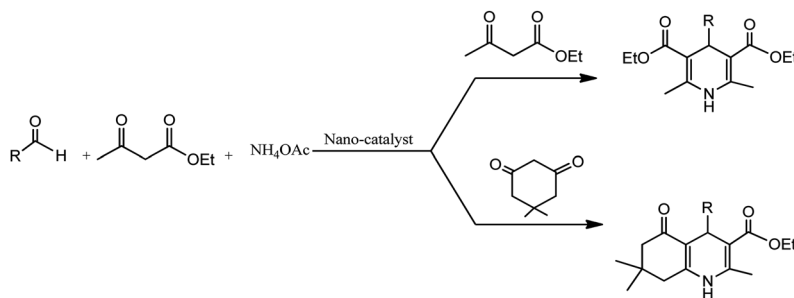
Table 3 Functionalized silica nanoparticle/support-catalyzed synthetic protocol of 1,4-DHP and its derivatives<sup>a</sup>



Entry	Catalyst	Temperature (°C)/Ultrasonic probe (W)	Solvent	Time	Yield <sup>b</sup> (%)	Ref.
1	Ultrasound SnCl <sub>4</sub> @nano-SiO <sub>2</sub>	40	EtOH	5 min	96	50
2	$[\beta\text{CD/Im}](\text{OTs})_2$ -silica	90	Solvent free	15 min	98	51
3	SO <sub>3</sub> H-KIT-5	Room temperature	Solvent free	60 min	87	52

<sup>a</sup> Reaction conditions: aldehyde (1.0 mmol), NH<sub>4</sub>OAc (1–1.5 mmol), dimedone (2.0 mmol). <sup>b</sup> Isolated yields.



Table 4 Magnetic nanoparticles/functionalized magnetic nanoparticles-catalyzed synthesis of 1,4-DHP<sup>a</sup>

Entry	Catalyst	Temperature (°C)/ Ultrasonic Probe(W)	Solvent	Time (min)	Yield <sup>b</sup> (%)	Ref.
1	$\gamma$ -Fe <sub>2</sub> O <sub>3</sub> , MW, and fixed bed flow reactor	100	Solvent free	5	93.5	69
2	$\gamma$ -Fe <sub>2</sub> O <sub>3</sub> @HAp@Melamine	80	Solvent free	15	94	70
3	Fe <sub>3</sub> O <sub>4</sub> /SiO <sub>2</sub> -PDA NPs/USW	Room temperature	EtOH	10	89	71
4	AIL-SCMNPs	60	Solvent free	10	92	72
5	Ultrasound Fe <sub>3</sub> O <sub>4</sub> @SiO <sub>2</sub> -SnCl <sub>4</sub>	40	EtOH	5	98	73
6	Fe <sub>3</sub> O <sub>4</sub> @SiO <sub>2</sub> @ADMPT/HPA nano catalyst	70	EtOH	35	92	74
7	NiFe <sub>2</sub> O <sub>4</sub> @SiO <sub>2</sub> -H <sub>14</sub> NaP <sub>5</sub> W <sub>30</sub> O <sub>110</sub>	120	Solvent free	10	94	75
8	Nano ZnFe <sub>2</sub> O <sub>4</sub>	Room temperature	H <sub>2</sub> O	30	90-96	76
9	(a) Hal-Fe <sub>3</sub> O <sub>4</sub> with 1,3-ketoesters (b) Hal-Fe <sub>3</sub> O <sub>4</sub> with dimedone	Reflux	EtOH	20	96 94	77
10	Fe <sub>3</sub> O <sub>4</sub> @IG	Ultrasound	EtOH	50	88	78
11	(a) $\gamma$ -Fe <sub>2</sub> O <sub>3</sub> @Cu@cellulose for 1, 4-dihydropyridine derivatives (b) $\gamma$ -Fe <sub>2</sub> O <sub>3</sub> @Cu@cellulose for polyhydroquinoline derivatives	Room temperature	Solvent free	Completion of reaction	80-92	79
12	Nano-FGT	100-120	Solvent free	35	80-91	87
13	Fe-C-O-Mo alloy	Reflux	EtOH	150	92	88
14	Chitosan NPs	80	Solvent free	20	90	89
15	Fe <sub>3</sub> O <sub>4</sub> @chitosan	Room temperature	EtOH	30-140	84-98	90
16	MGCS	Reflux	EtOH	15	84-89	91

<sup>a</sup> Reaction conditions: aldehyde (1.0 mmol), ethyl acetoacetate (2.0 mmol), NH<sub>4</sub>OAc (1-1.5 mmol), dimedone (2.0 mmol). <sup>b</sup> Isolated yields.

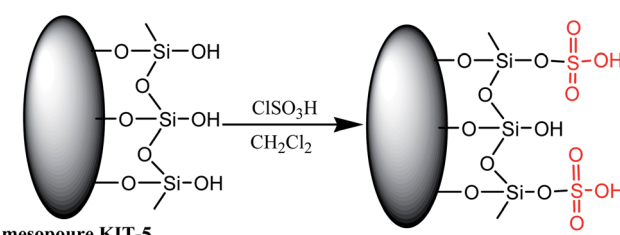
conditions, short reaction times, clean reaction profiles, and high yields.<sup>51</sup>

Mesoporous silica KIT-5, owing to its three-dimensional pore size and high surface area, serves as an ideal support for designing efficient catalysts. An inorganic-organic hybrid nanocatalyst, silica-bonded sulfuric acid on KIT-5 support, was efficaciously achieved by the reaction of KIT-5 with chlorosulfonic acid (Scheme 7) and was used to carry out the synthesis of 1,4-dihydropyridine derivatives (Table 3; entry 3).

To monitor the catalytic efficiency of SO<sub>3</sub>H-KIT-5 nanoparticles, the reaction of dimedone, aldehyde, NH<sub>4</sub>OAc, and ethyl acetoacetate in the presence of SO<sub>3</sub>H-KIT-5 was carried out at room temperature, which gave the desired products in excellent yields. The catalyst was readily recoverable and reusable up to five times with a non-appreciable loss of the activity. Along with this, easy separation, high surface area, high activity, and reaction in open air are some significant advantages that make mesoporous silica KIT-5 a suitable support for other nano-catalysts that are used for diverse organic transformations.<sup>52</sup>

## Magnetic nanoparticles/functionalized magnetic nanoparticle-catalyzed synthesis of 1,4-DHP

Although nanocatalysts possess several merits over conventional catalysts, due to their nanoscopic size, their recoverability from the reaction mixture is always a tedious process, thus hampering the economic and sustainability aspects of nano-scale protocols.<sup>53,54</sup> In this direction, over the last few years,

Scheme 7 Synthesis of the SO<sub>3</sub>H-KIT-5 nanocatalyst.

various magnetically-separable nanocarriers have been developed to avoid the inevitable loss of the catalyst during tedious recycling processes *via* filtration and centrifugation.<sup>55,56</sup> These nanoparticles and nanocarriers, owing to their insolubility and paramagnetic nature, ensure easy separability and recycling of the catalyst using an external magnet, thereby enhancing product purity and optimizing the operational cost.<sup>57-59</sup> Iron oxides including maghemite ( $\gamma$ -Fe<sub>2</sub>O<sub>3</sub>) and magnetite (Fe<sub>3</sub>O<sub>4</sub>), due to their inherent biocompatibility and ease of post-synthetic surface modification, have been extensively used for this purpose.<sup>60-65</sup> To improve the catalytic stability by overcoming the problems of agglomeration, these magnetic nanoparticles have been modified by coating with eco-friendly substances such as chitosan, cellulose, and silica.<sup>66,67</sup> Recently, the immobilization of ionic liquids on these magnetic nanoparticles has also been developed so that the favorable catalytic properties of liquids are transferred into the solid catalyst and separation issues associated with homogeneous ionic liquid are no longer there.<sup>68</sup>

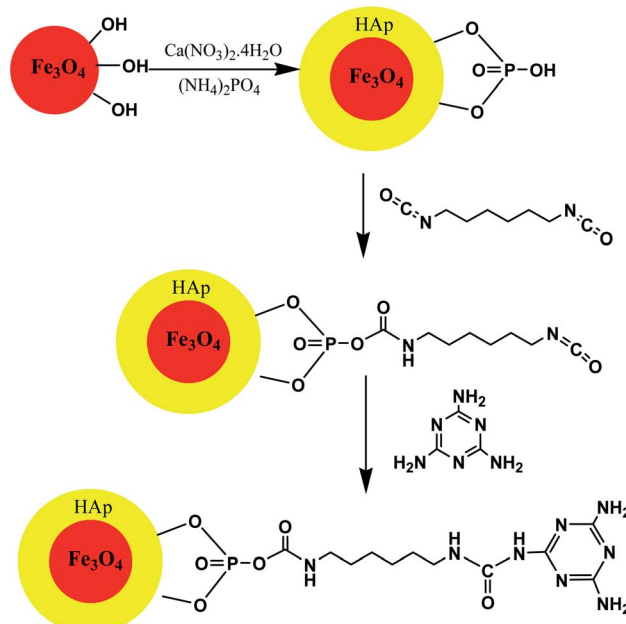
In this context,  $\gamma$ -Fe<sub>2</sub>O<sub>3</sub> nanoparticles were used in the condensation reaction of acetoacetic ester, araldehydes, and ammonia in novel designed micro-flow system under microwave irradiation (Table 4; entry 1). The optimization studies of the model reaction exhibited that the combination of the catalyst and the continuous micro-flow system under microwave irradiation at 100 °C for a few minutes afforded excellent yield and selectivity. Comparative studies on different heating methods (air, oil, and microwave) revealed the superiority of the continuous micro-flow system under microwave over air and oil bath heating in terms of the selectivity and yield with the least by-product formed due to the constant removal of the side products and desired products from the metal oxide surfaces. The better performance of the homemade catalysts compared to the commercially available catalysts was attributed to its more uniform and comparatively smaller size.<sup>69</sup>

In this context, hydroxyapatite encapsulated- $\gamma$ -Fe<sub>2</sub>O<sub>3</sub> nanoparticles functionalized with melamine were synthesized according to Scheme 8. The catalytic activity of the  $\gamma$ -Fe<sub>2</sub>O<sub>3</sub>@HAp@Melamine nanocatalyst was explored for the synthesis of 1,4-dihydropyridine and polyhydroquinoline derivatives under neat thermal conditions. This heterogeneous catalyst gave more than 94% yield in solvent-free conditions at 80 °C and was easily recoverable *via* magnetic decantation and was reusable several times with the retention of its catalytic activity (Table 4; entry 2). The method offered the development of greener and eco-compatible technology due to a cleaner reaction profile, operational simplicity, high yields, and recyclability of the catalyst as well as minimum pollution of the environment.<sup>70</sup>

In another report, different derivatives of 1,4-dihydropyridine (1,4-DHP) were synthesized in the presence of pyrimidine-2,4-diamine-functionalized magnetic nanoparticles. The nanocatalyst (Fe<sub>3</sub>O<sub>4</sub>/SiO<sub>2</sub>-PDA) was prepared by the coating of silica network (SiO<sub>2</sub>) and trimethoxy vinylsilane (TMVS) on Fe<sub>3</sub>O<sub>4</sub> nanoparticles, followed by functionalization with pyrimidine-2,4-diamine (PDA). The performance of the reported catalyst under microwave (MW), reflux, and ultrasound wave (USW) irradiations was comparatively examined. It was realized that

the most appropriate reaction condition was ultrasonication at 50 KHz in aqueous media for 2 h at 50 °C. The collaborative catalytic effect between the nanoparticles and USWs was studied carefully and the results in the form of good yields (89%) and short time (10 min) confirmed the extensive synergistic effect amongst the catalyst -NH<sub>2</sub> groups (as dynamic catalytic sites) and ultrasound waves (Table 4; entry 3). This synergistic effect resulted in close size distribution of the particles, excellent functionalization of the surface, particle uniformity, and great inhibition of particle aggregation. According to the chemical point of view, there is probable acceleration in the electronic resonance in the conjugated system of the loaded PDA's structure *via* USW's frequent irradiations, thus enhancing the bond formation ability of the present nitrogen atoms. The physical aspect clarifies that the USW irradiation offered a wider active surface area for reaction catalysis through the nanoparticle dispersion in the reaction mixture. Higher yields were attained on simultaneously applying both magnetic nanoparticles and USW irradiation rather than using the nano-catalyst alone. The results of energy-dispersive spectroscopy showed a significant peak intensity of the Si atom, proving the preservation of the nanoparticles' core structure during ultrasonication. In this study, it has been proven that particle accumulation was also prevented by ultrasonication. In addition, the MW irradiation method showed the occurrence of physical adsorption.<sup>71</sup>

Another environmentally benign catalyst, magnetite nanoparticles reinforced with a novel acidic ionic liquid, was synthesized and used for preparing polyhydroquinoline and 1,4-dihydropyridine derivatives *via* symmetric and asymmetric Hantzsch reactions under neat conditions (Table 4; entry 4). The recovered catalyst was used for at least five runs with an



Scheme 8 Synthetic procedure for the  $\gamma$ -Fe<sub>3</sub>O<sub>4</sub>@HAp@Melamine nanoparticles.





Fig. 4 TEM image of  $\text{SnCl}_4$ -functionalized nano- $\text{Fe}_3\text{O}_4$  encapsulated-silica nanoparticles ( $\text{Fe}_3\text{O}_4@\text{SiO}_2-\text{SnCl}_4$ ). Adapted with permission from ref. 73. Copyright Royal Society of Chemistry.

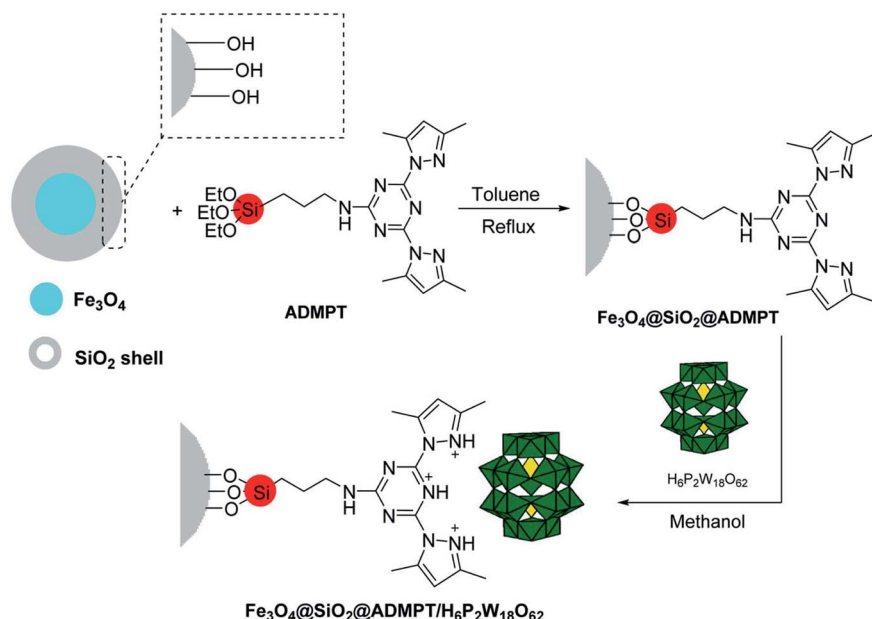
insignificant loss in the catalytic activity. Simple operation, high efficiency, shorter reaction time, and environment friendliness are the special highlights of this new catalyst.<sup>72</sup>

The ultrasound aided synthesis of 1,4-DHP derivatives was developed using  $\text{Fe}_3\text{O}_4@\text{SiO}_2-\text{SnCl}_4$  as a novel heterogeneous acidic nano-catalyst. The  $\text{SnCl}_4$ -functionalized nano- $\text{Fe}_3\text{O}_4$  encapsulated-silica nanoparticles were well-characterized by XRD, VSM, SEM, and TEM analysis (Fig. 4). During optimization studies, the reactivity of the catalyst was established by condensation reaction between dimedone, benzaldehyde,  $\text{NH}_4\text{OAc}$ , and ethyl acetoacetate in the presence of various solvents and catalyst loadings under reflux and ultrasonication conditions. Studies demonstrated that EtOH was the best solvent for the reported catalyst in USWs. Ultrasound irradiation (40 W) in addition to the excellent yield in lesser time

offered mild reaction conditions with operational simplicity in comparison to the refluxing method. It was found that 1,3-dicarbonyl compounds reacted successfully with aromatic aldehydes having either electron-withdrawing or electron-donating substituents to attain the corresponding 1,4-dihydropyridines in excellent yields (Table 4; entry 5). The catalyst was reusable up to five times without an appreciable loss of its catalytic properties. There is no considerable change found in its magnetic properties after being recovered from the reaction mixture. The minimum leaching of the catalyst in this protocol suggests the stability of the nano-catalyst under ultrasound irradiation. The recyclability, low toxicity, low cost, and eco-friendliness of the catalyst are some notable contributions of the presented method in the field of one-pot multicomponent Hantzsch reaction.<sup>73</sup>

The use of heteropolyacids as catalysts has been explored recently due to their versatile properties and advantages over conventional inorganic acids catalysts. An eco-friendly nano-hybrid catalyst was synthesized by the chemical fastening of  $\text{H}_6\text{P}_2\text{W}_{18}\text{O}_{62}$  (Wells-Dawson heteropolyacid) on the surface of functionalized  $\text{Fe}_3\text{O}_4$  nanoparticles with the ADMPT [2,4-bis(3,5-dimethylpyrazol)-triazine] linker, as shown in Scheme 9.

A safe, cost effective, convenient, and novel protocol for the preparation of 1,4-dihydropyridine derivatives was developed through the single-pot reaction of acetoacetic ester, substituted aromatic aldehydes,  $\text{NH}_4\text{OAc}$ , and the reported nano-hybrid catalyst in ethanol at 70 °C for 35 min, leading to high product yields. A separate comparative study was conducted for the catalytic activity of  $\text{Fe}_3\text{O}_4@\text{SiO}_2$ ,  $\text{Fe}_3\text{O}_4@\text{SiO}_2@\text{ADMPT}$ , and  $\text{Fe}_3\text{O}_4@\text{SiO}_2@\text{ADMPT}/\text{H}_6\text{P}_2\text{W}_{18}\text{O}_{62}$  nano-catalyst, which exhibited that although the components of the nano-hybrid showed trace activity, the aforesaid catalyst gave excellent yields in the desired organic synthesis, indicating that the anchoring



Scheme 9 Synthetic procedure for the  $\text{Fe}_3\text{O}_4@\text{SiO}_2@\text{ADMPT}/\text{H}_6\text{P}_2\text{W}_{18}\text{O}_{62}$  nano-catalyst. Adapted with permission from ref. 74. Copyright Taylor & Francis Group.



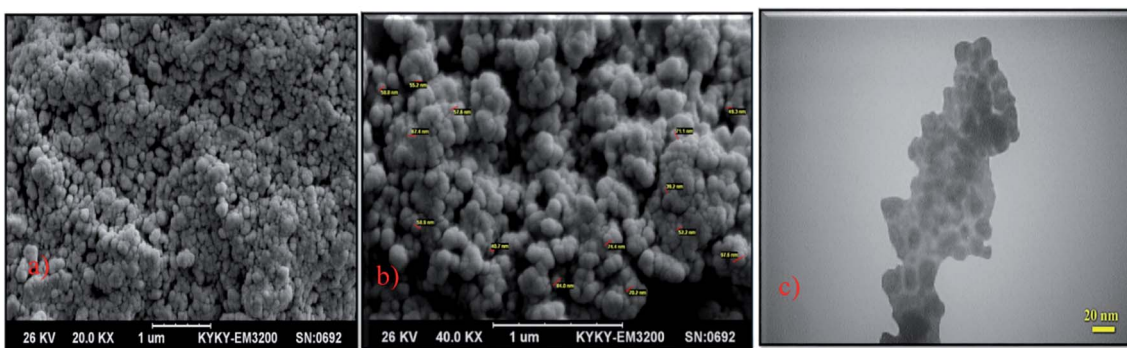


Fig. 5 (a) & (b) SEM and (c) TEM images of the  $\text{Fe}_3\text{O}_4@\text{GA}@\text{IG}$  nanoparticles. Adapted with permission from ref. 78. Copyright Royal Society of Chemistry.

of the heteropolyacid onto the modified solid material  $\text{Fe}_3\text{O}_4@\text{SiO}_2@\text{ADMPT}$  surface was responsible for a drastic increase in its catalytic activity (Table 4; entry 6). It was also found that the electron-withdrawing group in benzaldehyde enhanced the rate of the reaction, while the effect was reversed in the case of electron-donating groups in benzaldehyde. The nano-catalyst was easily separated from the products *via* an external magnet and was successfully reusable for five consecutive runs without any considerable loss of the activity. This protocol has become a useful and attractive method for the synthesis of 1,4-DHPs due to advantages such as excellent product yields, use of inexpensive and non-toxic materials, magnetic recyclability, milder reaction conditions, environment friendliness, and simple procedure with short reaction times.<sup>74</sup>

Preyssler heteropolyacid ( $\text{H}_{14}\text{NaP}_5\text{W}_{30}\text{O}_{120}$ ) is considered as a remarkable support material due to its remarkable properties such as high thermal and hydrolytic stability, low surface area, acidic protons, and high solubility in polar solvents. Therefore, preyssler heteropolyacid ( $\text{H}_{14}\text{NaP}_5\text{W}_{30}\text{O}_{120}$ ) was supported on magnetic  $\text{NiFe}_2\text{O}_4$  for the preparation of silica-coated magnetic nanoparticles-supported heteropolyacid ( $\text{NiFe}_2\text{O}_4@\text{SiO}_2-\text{H}_{14}[\text{NaP}_5\text{W}_{30}\text{O}_{110}]$ ). These nanohybrids have shown to be versatile and highly efficient heterogeneous catalysts for the one-pot four-component cyclocondensation to 1,4-dihydropyridine derivatives using a mixture of ethyl acetoacetate, aldehyde, cyclohexane-1,3-dione or dimedone, and  $\text{NH}_4\text{OAc}$  or aromatic aniline (Table 4; entry 7). The synthesized catalyst was magnetically recovered and reused four times without an appreciable loss in its catalytic efficiency. Further, the scope and generality of this four-component one-pot Hantzsch synthesis was examined by taking different aldehydes and 1,3-dicarbonyl compounds. All the reactions progressed well within 10–60 min at 120 °C under neat conditions to afford the polyhydroquinoline derivatives in good to excellent yields.<sup>75</sup>

A Lewis acid-based magnetic nano  $\text{ZnFe}_2\text{O}_4$  powder was used to condense aldehydes,  $\text{NH}_4\text{OAc}$ , and ethyl acetoacetate *via* multicomponent synthesis to afford 1,4-dihydropyridine derivatives using water as the solvent. In the optimization studies, different solvents such as EtOH, acetonitrile, and  $\text{H}_2\text{O}$  were studied and their efficiency was established. It was observed in the presence of the nano  $\text{ZnFe}_2\text{O}_4$  powder and the aqueous

medium afforded the corresponding 1,4-dihydropyridine derivatives in good yield at room temperature. The advantages of the present protocol using  $\text{ZnFe}_2\text{O}_4$ -NPs over  $\text{Fe}_3\text{O}_4@\text{SiO}_2$  and  $\text{CuFe}_2\text{O}_4$  catalyzed protocols are the higher product yield and shorter reaction times under similar conditions (Table 4; entry 8). In addition, inexpensive, highly effective, stable, recyclable, moisture-resistant, and reusable up to five times with the same efficacy are some of the other advantages.<sup>76</sup>

The unique feature of halloysite such as outstanding biocompatibility and unique morphology encouraged scientists to investigate it for use in nano-composite materials with magnetic metal oxide nanoparticles in order to synthesize thermally stable, crystalline magnetic halloysite ( $\text{Hal}-\text{Fe}_3\text{O}_4$ ) nanocomposite. The prepared nanocomposite was used to catalyze Hantzsch reaction so as to prepare 1,4-dihydropyridines (Table 4; entry 9). A mixture of dimedone,  $\text{NH}_4\text{OAc}$ , and benzaldehyde were refluxed in the presence of the reported nanocomposite in EtOH for 20 min and the pure product was obtained in good yields under the optimized conditions. The presence of electron-donating or withdrawing group-substituted aldehydes with dimedone had little or no effect on the reaction time and yield. It was reported that the loading of iron oxide on halloysite to give the nanocomposite increased the reaction efficiency remarkably (94% yield) as the experiments taking iron oxide nanoparticles and halloysite separately afforded a very low amount of the desired product. Mild operation conditions, high efficiency, easy work-up procedure, green reaction media, and using readily available green aluminosilicate materials with excellent recovery and reusability for eight successive cycles without much loss in the efficiency are some of the advantages of this study.<sup>77</sup>

In another report, biocompatible core/shell magnetic nanoparticles  $\text{Fe}_3\text{O}_4@\text{GA}@\text{IG}$  were synthesized *via* the coating of isinglass (IG) in the presence of glutaraldehyde as the linking agent. The reported  $\text{Fe}_3\text{O}_4@\text{GA}@\text{IG}$  nanoparticles were characterized by TEM, SEM, and XRD techniques (Fig. 5).

The catalytic potential of the  $\text{Fe}_3\text{O}_4@\text{GA}@\text{IG}$  nanoparticles was evaluated in the preparation of 4H-pyran and 1,4-dihydropyridine derivatives under sonication in EtOH. To attain the optimal conditions, the model reactions were carried out at different parameters such as catalyst loading, temperature,



energy sources, and solvent. Also, the synergistic effect of the ultrasound was thoroughly studied, which revealed that the use of ultrasound decreased the reaction time and increased the yields remarkably (Table 4; entry 10). The catalytic efficacies of the prepared nanohybrid were compared with its individual components (IG and  $\text{Fe}_3\text{O}_4$ ) to reveal that the hybrid system led to higher yields at short reaction times and demonstrated high activity.<sup>78</sup>

A new protocol has been demonstrated to prepare polyhydroquinolines and 1,4-dihydropyridines in high yields using biopolymer-based magnetic nanocomposite  $\gamma\text{-Fe}_2\text{O}_3@-\text{Cu@cellulose}$  as the catalyst. Considering 4-chlorobenzaldehyde,  $\text{NH}_4\text{OAc}$ , and ethyl acetoacetate/dimedone (for polyhydroquinoline) as the model substrates, the reaction conditions were optimized to reveal that the presence of the catalyst in solvent-free condition seems the best to provide the corresponding products in excellent yield (Table 4; entry 11). The reactivity of various aldehydes was also monitored and it was found that the aldehydes possessing electron-releasing groups reacted well to give moderately high yields of the products in shorter time as compared to the aldehydes bearing electron-withdrawing group. Further, the catalytic effects of  $\gamma\text{-Fe}_2\text{O}_3$ ,  $\gamma\text{-Fe}_2\text{O}_3@-\text{Cu}$ , and  $\gamma\text{-Fe}_2\text{O}_3@-\text{Cu@cellulose}$  were compared and it was deduced that there was a considerable increase in the catalytic activity after the loading of  $\gamma\text{-Fe}_2\text{O}_3@-\text{Cu}$  on cellulose, while sufficient catalytic activity was hardly displayed in the presence of basic cellulose. The role of Cu nanoparticles was more important along with  $\gamma\text{-Fe}_2\text{O}_3$ . Their synergistic effect appeared when both of these together

( $\text{Fe}_2\text{O}_3@-\text{Cu}$ ) were coated on the biopolymer. Some remarkable features of this work are the innovative development of a bio-nanostructure with low-leaching properties, easy separability and reusability, without losing its efficacy after at least five cycles, ease of work-up procedure, under moderate and green conditions.<sup>79</sup>

Organocatalysts are usually homogeneous in nature but when modified as nano-catalysts, they are found to possess heterogeneous catalytic behavior.<sup>80,81</sup> Various organic moieties such as L-proline, glutathione, cyclodextrins, vitamin B1, meglumine, and chitosan are natural and non-toxic, and thus have been exploited as organocatalysts in the regioselective and stereoselective synthesis of various biologically important organic compounds.<sup>82-84</sup> Their greener fabrication represents eco-friendly alternatives to toxic acidic/basic catalysts. Therefore, the heterogenization of active molecules such as amino acids or organic moieties with a magnetic nano-solid support is not only an environment friendly but at the same time an efficient strategy to achieve the easy recovery and recyclability of the catalyst.<sup>85,86</sup> Also, organo-nano catalysts offer extra benefits such as high yield, magnetically-aided catalyst, recyclable, reusable, and maximum utilization by dispersing it over an increased surface area, which resulted in the increased efficiency of the overall catalytic process.

In this context, a convenient and eco-friendly method was developed to prepare magnetic  $\text{Fe}_3\text{O}_4$ -supported glutathione as an organic nano-catalyst, which showed excellent catalytic activity in the multicomponent synthesis of 1,4-DHP derivatives. Under neat conditions, the nano-FGT catalyst introduced

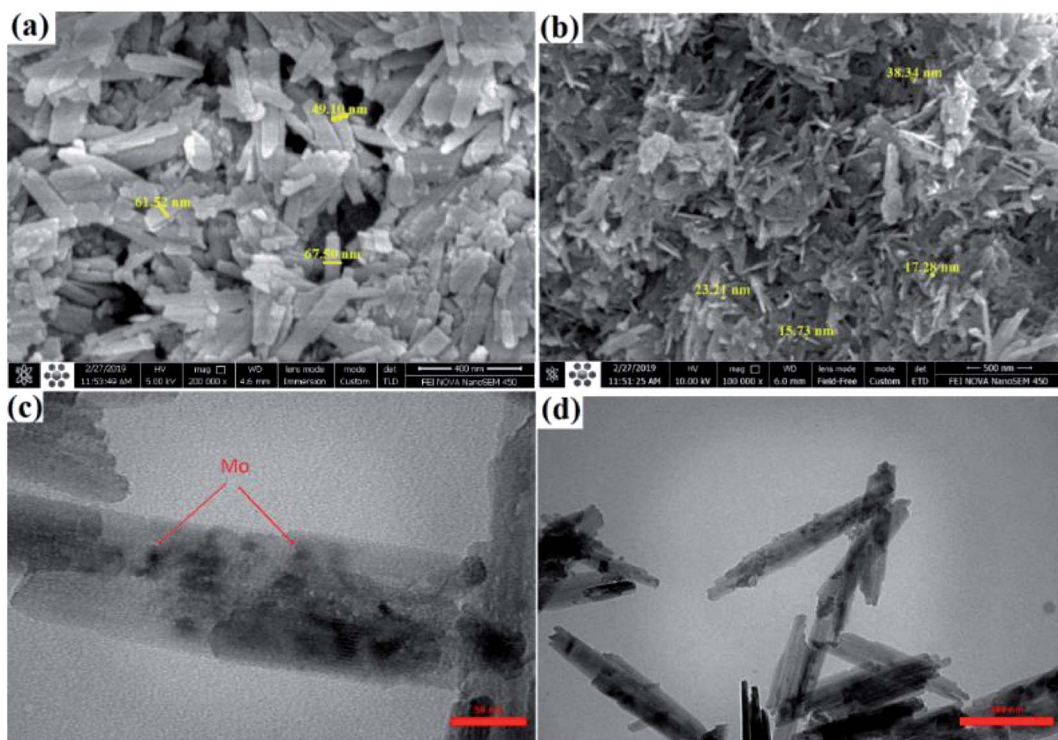


Fig. 6 (a) & (b) SEM; (c) & (d) TEM images of Fe-C-O-Mo nano-rods. Adapted with permission from ref. 88. Copyright Clearance Center's RightsLink® service, Elsevier.



into a mixture of benzaldehyde, ethyl acetoacetate, dimedone, and  $\text{NH}_4\text{OAc}$  at 100–120 °C was found to be sufficient to give high yields of 1,4-dihydropyridine derivatives (Table 4; entry 12). The nature and position of the substituents on aldehyde did not show any effect on the reaction efficiency. The reusability and recovery of the catalyst was studied extensively and it was found that after reaction completion, the catalyst was separated using an external magnet and was reusable for up to six times with the same productivity. Investigations to determine catalyst leaching from the support suggested that there was low leaching of glutathione, which showed the stability of the catalyst. Other major advantages of the synthetic protocol are good yields, easy catalyst handling, shorter reaction times, and high stability of the catalyst along with simple work-up processes, making it a sustainable and economical method.<sup>87</sup>

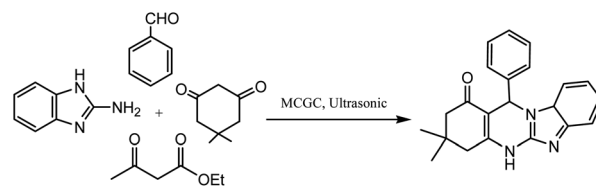
A green and economical method from the industrial aspect has been developed where magnetic Fe–C–O–Mo nano-rods have been synthesized from waste metal precursor (a cheap screw) by a new and efficient top-down protocol (Fig. 6). The synthesized magnetic Fe–C–O–Mo nano-rods were applied towards the efficient preparation of Hantzsch dihydropyridine and Biginelli dihydropyrimidone compounds under moderate conditions.

Under the optimized conditions, a mixture of benzaldehyde, acetoacetic ester, and  $\text{NH}_4\text{OAc}$  was stirred magnetically under reflux conditions in EtOH in the presence of Fe–C–O–Mo nanorods (0.1 mol% Mo), which gave excellent yields (Table 4; entry 13). Various aldehydes (electron rich or electron deficient) could be condensed efficiently to the corresponding dihydropyridines with good to high yields. To find out the actual active catalytic site, a model reaction was carried out in the presence of coke and  $\text{Hg}(0)$  as a poisoning and deactivating reagent, which resulted in a reduction of the catalytic activity, confirming that the observed catalytic behavior of the Fe–C–O–Mo nano-rods was due to the molybdenum metal doped in the nanoscale-sized structure. A control experiment taking  $\text{Fe}_3\text{O}_4$  nanoparticles as the catalyst in the model reaction under the optimized conditions demonstrated a trace or undetectable product after long reaction time, ruling out the possibility of any synergistic effect, thus further confirming the fact that the Mo sites are responsible for the observed catalytic activity. The catalyst represented very high recyclability and stability even after eight consecutive runs with a negligible decrease in the efficiency without the sign of any metal leaching.<sup>88</sup>

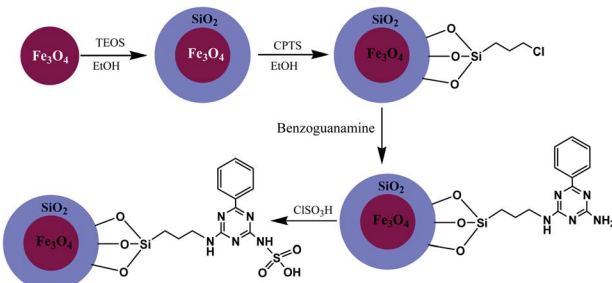
Chitosan is a bactericidal, biocompatible, eco-friendly natural material with notable surface modification potential owing to the presence of hydroxyl and amino functional groups on its structure. It has the capability to activate the reaction by means of hydrogen bonding and lone pairs. These chitosan particles, consisting of active hydroxyl and amino groups, can be further chemically modified into different forms that can provide greater support to a variety of catalytic species with enhanced efficacy. In this context, chitosan nanoparticles, prepared by the gelation process of chitosan, are used to catalyze the Hantzsch reaction. The less sterically-hindered and electron-withdrawing groups containing araldehydes displayed better results than the sterically-hindered and electron-

releasing group containing araldehydes. With improved catalytic efficiency compared to bulk chitosan, the present procedure offers a straight-forward and quick method for the preparation of 1,4-DHPs with enhanced yields under greener conditions and shorter reaction time without the use of expensive reagents (Table 4; entry 14).<sup>89</sup> Further incorporating the advantages of chitosan along with magnetic nanoparticles, a greener nanocomposite,  $\text{Fe}_3\text{O}_4@\text{chitosan}$  was prepared and used to synthesize biologically important dihydropyridine derivatives through a green and inexpensive method *via* the four-component reaction of a mixture of various aromatic aldehydes, 1,3-cyclohexandione or dimedone, ethyl/methyl acetoacetate, and  $\text{NH}_4\text{OAc}$  (Table 4; entry 15).<sup>90</sup> The same group of scientists reported the synthesis of another magnetic guanidinylated chitosan nano-bio composite (MGCS) through the surface modification of chitosan by the introduction of more amino groups from guanidine. Due to the magnetic properties and large number of amino groups of the synthesized nano-bio composites, it was successfully utilized as a heterogeneous catalyst for the synthesis of 1,4-dihydropyridines using a mixture of  $\beta$ -ketoester, benzaldehyde, and  $\text{NH}_4\text{OAc}$  under the same optimized reaction conditions as that used in the previous protocol (Table 4; entry 16). The present method has several advantages such as the reusability of the catalyst for at least seven runs without any decrease in its activity, excellent yields, simple work up, and mild reaction conditions.<sup>91</sup>

Magnetic cyanoguanidine-modified chitosan (MCGC), an eco-friendly retrievable nano-catalyst, was prepared and utilized in 1,4-DHP synthesis through the condensation of the substituted aromatic aldehydes, ethyl acetoacetate, and  $\text{NH}_4\text{OAc}$  in ultrasonic irradiation and reflux conditions

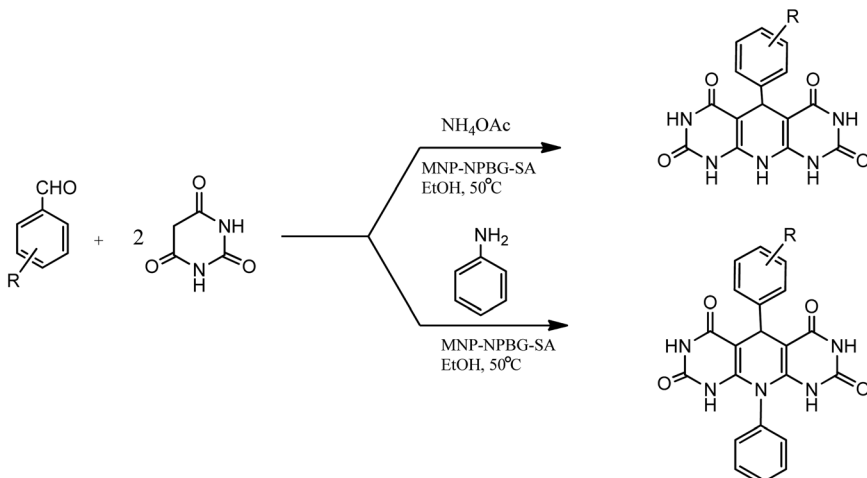


Scheme 10 Magnetic cyanoguanidine-modified chitosan nano-catalyst-assisted synthesis of 1,4-DHP-containing derivatives under ultrasonic conditions.



Scheme 11 Synthesis of *N*-propylbenzoguanamine sulfonic acid stabilized on silica-coated nano- $\text{Fe}_3\text{O}_4$  nanoparticles.





**Scheme 12** MNP-NPBG-SA-assisted synthesis of 1,4-DHP derivatives in ethanol solvent.

(Scheme 10). Taking a model reaction into consideration, the effect of the irradiation frequency, solvent, temperature, and catalyst load was studied, and the optimum reaction conditions ascertained were 30–32 °C bath temperature, 25 kHz irradiation frequency, and EtOH as the best solvent. The high purity of the products, shorter time, and excellent yields are some of the factors that make ultrasonic irradiation better compared to refluxing conditions. The usefulness of this method lies in its benefits such as short reaction times, low catalyst loading, milder reaction conditions, easy work-up procedure, compatibility with varied range of substituted aromatic aldehydes, and reusability up to eight consecutive cycles.<sup>92</sup>

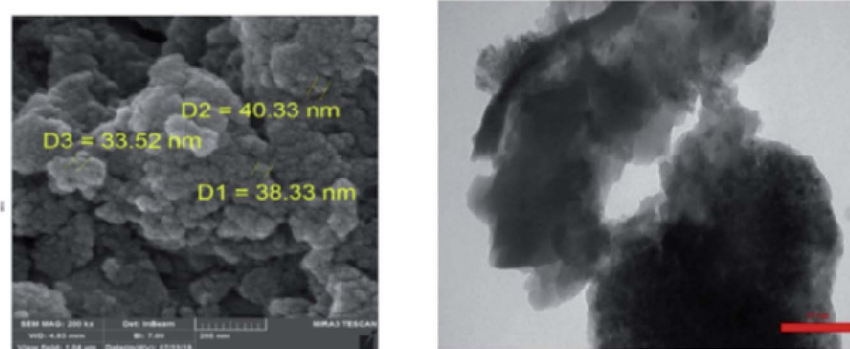
Magnetic nanoparticles with *N*-propylbenzoguanamine sulfonic acid immobilized on silica-coated nano- $\text{Fe}_3\text{O}_4$  particles (MNP-NPBG-SA), as a novel and effective catalyst with good recyclability and reusability, was synthesized (Scheme 11) and utilized in the preparation of 1,4-dihydropyridine derivatives.

Under the optimized conditions, the reaction of aromatic aldehyde, barbituric acid, and aniline or  $\text{NH}_4\text{OAc}$  was successfully carried out in the presence of MNP-NPBG-SA in EtOH at 50 °C with excellent product yield (Scheme 12). The substituted aromatic aldehydes with electron-withdrawing or electron

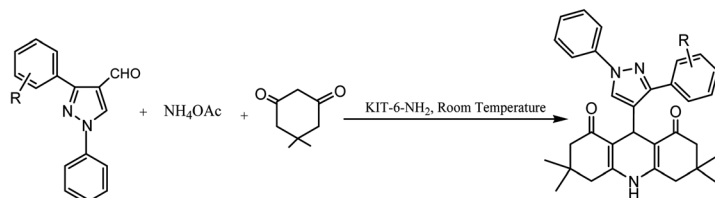
donating groups reacted with barbituric acid and  $\text{NH}_4\text{OAc}$ /aniline to afford the corresponding products in excellent yields. The catalytic activity of the catalyst was examined for five runs, which showed a slight decrease may be because of the non-recovery of some of the nanoparticles by the external magnet or the chemical poisoning of the catalyst's surface during reaction. After consecutive five runs, no distinctive structural changes were observed in the recovered catalyst in comparison to the unused catalyst.<sup>93</sup>

Schiff-base/copper complex fixed on amine-functionalized mesoporous silica (KIT-6-NH<sub>2</sub>) magnetic nanoparticles was synthesized and characterized (Fig. 7).

The synthesized  $\text{Fe}_3\text{O}_4@\text{SiO}_2@\text{KIT-6}@\text{Schiff-base}$  complex nanoparticles were used as the nano-catalyst for the synthesis of different 1,4-dihydropyridine derivatives *via* the one-pot three-component cyclo-condensation reaction of various aldehydes, dimedone, and  $\text{NH}_4\text{OAc}$  in aqueous media (Scheme 13). Furthermore, after reaction completion, the recycling potential of the catalyst *via* magnetic separation was tested and the catalyst was found to possess exceptional recyclability for up to six runs without any loss in its apparent features. The exceptionally high yields of the products, operational simplicity, easy



**Fig. 7** (a) SEM and (b) TEM images of the  $\text{Fe}_3\text{O}_4@\text{SiO}_2@\text{KIT-6}@\text{Schiff-base}$  complex. Adapted with permission from ref. 94. Copyright Clearance Center's RightsLink® service, Elsevier.

Scheme 13 Magnetic nanoparticles KIT-6-NH<sub>2</sub>-assisted synthesis of 1,4-DHP derivatives.

means of catalyst separation and recyclability, high selectivity, greenness, and waste reduction are the key benefits of this synthetic method.<sup>94</sup>

## Nano-zeolites catalyzed synthesis of 1,4-DHP

Poly(vinylimidazolium acetic acid) was coated on clinoptilolite nano-zeolite for the preparation of a novel heterogeneous acidic catalyst, NZ@PIL-COOH. This nanocomposite's activity as a catalyst was explored for the synthesis of 1,4-DHP and polyhydroquinolines. For this, a mixture of malononitrile, various aldehydes, dimedone, and NH<sub>4</sub>OAc in the presence of the reported nanocomposite were carried out at 60 °C to give polyhydroquinolines. The solid acid catalyst exhibited high reactivity, stability, very high conversion rates, easy recoverability, and reusability for up to five cycles with the maintained catalytic activity. The present methods' suitability was demonstrated through the comparative study of different acid catalysts, namely, melamine trisulphonic acid, PPA-SiO<sub>2</sub>, Nano-ZrO<sub>2</sub>-SO<sub>3</sub>H, Nano-Fe<sub>3</sub>O<sub>4</sub>-TiO<sub>2</sub>-SO<sub>3</sub>H, Fe<sub>3</sub>O<sub>4</sub>@SiO<sub>2</sub>@NH-NH<sub>2</sub>-PW, *p*-dodecylbenzenesulphonic acid, CBSA, and Caro's acid-silica gel, which revealed that NZ@PIL-COOH was the most efficient catalyst in the solvent EtOH at 60 °C (Table 5; entry 1).<sup>95</sup>

The combination of pumice volcanic rock and cellulose matrix acts as a novel hybrid heterogeneous nanocomposite utilized as a biodegradable catalyst to assist in some important organic reactions. These nanocomposites and ultrasound waves work synergistically to obtain the 1,4-DHPs-containing

derivatives in good yields in lesser reaction times (Table 5; entry 2). The studies revealed that cellulose, along with its catalytic activity, acts as a matrix for the immobilization of pumice nanoparticles because of its microfiber structure. These properties are because of the hydrophobic interactions and strong van der Waals forces amongst the particles and the substrate.<sup>96</sup> In addition, it was found that the recovered nanoparticles showed no significant change in the structure due to their considerable structure stability. Evidence such as no change in the carbon elements' weight percentage and no jelly nature in the reaction environment proved the absence of cellulose leaching from the catalytic system during the reaction and recycling.

Boehmite due to its remarkable features like thermal and chemical stability, high specific surface area, cheap and commercial availability, high dispersity, air and moisture insensibility and easy modification makes it attractive solid-phase, recoverable and sustainable heterogeneous catalyst for a variety of multicomponent reactions. The 3,4-dihydropyrimidin-2-(1*H*)-ones and 1,4-DHP derivatives were prepared effectively with decent yields using silylpropyl sulfamic acid functionalized boehmite [BNPs@SiO<sub>2</sub>(CH<sub>2</sub>)<sub>3</sub>NHSO<sub>3</sub>H] nanoparticles at 70–80 °C in methanol/solvent free conditions (Table 5; entry 3). Moreover, the catalyst could be reused for at least five consecutive runs with only 7% reduction in yield.<sup>97</sup>

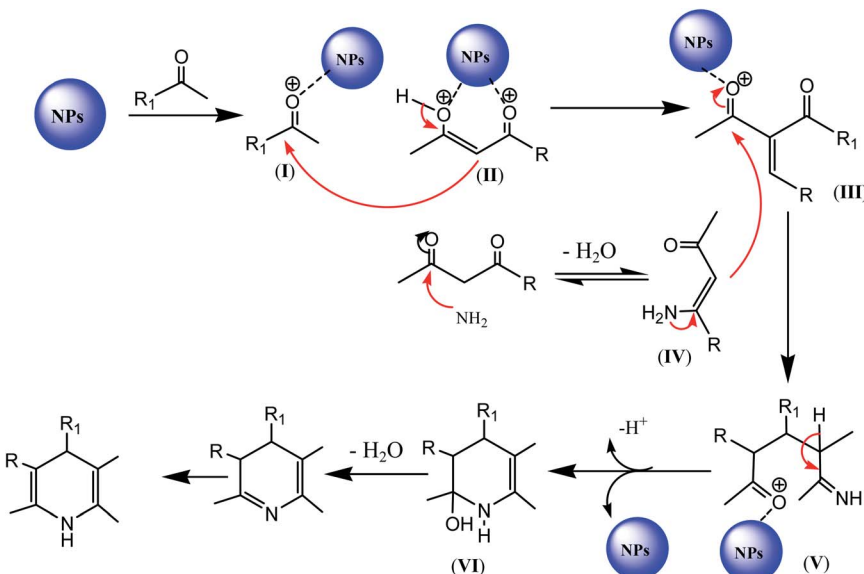
In another report, L-tyrosine-loaded polymeric nanoparticles (LTNP) were explored for the synthesis of Hantzsch 1,4-DHP-containing derivatives (Table 5; entry 4). The Eudragit®RS100 polymers coating properties such as swelling and flexibility are

Table 5 Nanoparticles supported on zeolite-catalyzed synthesis of 1,4-DHPs<sup>a</sup>

Entry	Catalyst	Temperature (°C)/Ultrasonic probe (W)	Solvent	Time (min)	Yield <sup>b</sup> (%)	Ref.
1	NZ-PIL-COOH	60	EtOH	20	98	95
2	Ultrasound cellulose/pumice nanocomposite	Room Temperature/(60 KHz,150)	EtOH	10	93–97	96
3	BNPs@SiO <sub>2</sub> (CH <sub>2</sub> ) <sub>3</sub> NHSO <sub>3</sub> H	70	EtOH	30	97	97
4	LTNPs	70	H <sub>2</sub> O	5	90	98

<sup>a</sup> Reaction conditions: arylaldehyde (1.0 mmol), ethyl acetoacetate (2.0 mmol), NH<sub>4</sub>OAc (1.0 mmol). <sup>b</sup> Isolated yields.





**Scheme 14** Reaction mechanism of the nanoparticle-catalyzed synthesis of 1,4-DHPs-containing derivatives.

responsible for enhancing the dispersion of L-tyrosine and increasing its catalytic activity. In another study, 1,4-DHP was attained in moderate yields in comparatively longer time on the reaction of ferrocenyl aldehydes and  $\beta$ -ketoesters in the presence of free L-tyrosine catalyst, whereas prominent progresses in both the yield and time were observed on the replacement of the amino acid by LTNP. As the ferrocene moiety has potential use in drugs, 1,4-DHPs with ferrocenyl side chains can be synthesized through fast, green, and much easier synthetic protocol, thus paving the way to the production of vital drug molecules on a large scale. High product yields are owed to enhanced penetrability of L-tyrosine into the reaction mixture, which in turn is due to the reduced particle size and increased surface area of LTNP. The noteworthy advantages of this reaction protocol include green methodology, improved surface area, easy catalyst separation, very small amount of catalyst, and easy dispersion of L-tyrosine through the thin polymer coat. Thus, this novel catalyst can be utilized in various green organic transformations.<sup>98</sup>

## General reaction mechanism of the nanoparticle-catalyzed synthesis of 1,4-DHPs-containing derivatives

In the literature, a general mechanism for nanomaterial-catalyzed synthesis of 1,4-dihydropyridine-containing compounds was suggested, in which initially, the nanoparticles activate diketone and aldehyde for nucleophilic attack to generate intermediate **III**. Intermediate **III** is further activated by the nanoparticles, thus facilitating the nucleophilic attack of **IV** to give another intermediate **V**. Intermediate **V** undergoes loss of proton to generate **VI** via cyclization, which is converted into the target 1,4-dihydropyridine moiety after few general steps, as depicted in Scheme 14.<sup>88</sup>

## Conclusion

1,4-Dihydropyridine and its derivatives are very useful heterocyclic motifs due to their biological and therapeutic values. The main goal of chemists is to augment the conventional Hantzsch reaction for the synthesis of 1,4-DHPs-containing compounds with the intent of improving the yield, lowering the temperature, minimizing the by-products, and designing economical and environmentally benign methodologies. Out of the several synthetic protocols reported so far for the preparation of 1,4-DHP derivatives since Hantzsch's invention, the utilization of different types of nanomaterials as heterogeneous catalysts is undoubtedly an eco-friendly and efficient methodology. This review article demonstrated the advantages of using various types of nanomaterials such as metal nanoparticles, metal oxides/mixed-metal oxides nanoparticles, magnetic nanoparticles, metal nano-clusters, organic inorganic nano-hybrids, nanoflakes, magnetic nanocomposites, nano bio-composites (using organic moieties such as cellulose, IG, and chitosan), and nanoparticles supported on mesoporous materials, zeolites under reflux, as well as ultrasound and microwave conditions in the synthesis of 1,4-DHP derivatives since 2015. We hope that the present review would surely motivate process researchers to develop green and novel synthetic routes to 1,4-DHPs, considering the various industrial and environmental concerns and the area of nanomaterial-catalyzed synthesis of DHPs will continue to thrive.

## Conflicts of interest

There are no conflicts of interest to declare.

## Acknowledgements

R. M. admiringly acknowledges Zakir Husain Delhi College, Delhi for laboratory facilities. R. S. acknowledges Manipal

University Jaipur, MNIT Jaipur for the assistance in data acquisition. R. N. acknowledges the infrastructural and laboratory facilities provided by S. S. Jain Subodh P. G. (Autonomous) College, Jaipur.

## References

- 1 S. Dang, H. Yang, P. Gao, H. Wang, X. Li, W. Wei and Y. Sun, *Catal. Today*, 2019, **330**, 61–75.
- 2 P. K. Tandon and S. B. Singh, *J. Catal. Catal.*, 2014, **1**, 1–14.
- 3 K. Yan, G. Wu, T. Lafleur and C. Jarvis, *Renewable Sustainable Energy Rev.*, 2014, **38**, 663–676.
- 4 H. Luo, H. Jiang, T. Klande, Z. Cao, F. Liang, H. Wang and J. Caro, *Chem. Mater.*, 2012, **24**, 2148–2154.
- 5 A. G. Atanasov, B. Waltenberger, E. Pferschy-Wenzig, T. Linder, C. Wawrosch, P. Uhrin, V. Temml, L. Wang, S. Schwaiger, E. H. Heiss, J. M. Rollinger, D. Schuster, J. M. Breuss, V. Bochkov, M. D. Mihovilovic, B. Kopp, R. Bauer, V. M. Dirsch and H. Stuppner, *Biotechnol. Adv.*, 2015, **33**, 1582–1614.
- 6 R. A. Khan, *Saudi Pharm. J.*, 2018, **26**, 739–753.
- 7 H.-A. S. Abbas, W. A. E. Sayed and N. M. Fathy, *Eur. J. Med. Chem.*, 2010, **45**, 973–982.
- 8 D. J. Triggle, *Cell. Mol. Neurobiol.*, 2003, **23**(3), 293–303.
- 9 M. D. Luca, G. Iolele and G. Ragno, *Pharmaceutics*, 2019, **11**, 85.
- 10 J. Briede, M. Stivrina, B. Vigante, D. Stoldere and G. Duburs, *Cell Biochem. Funct.*, 2008, **26**, 238–245.
- 11 K. Elumalai, M. Elumalai, K. Eluri, S. Srinivasan, M. A. Ali, B. V. Reddy and S. P. Sarangi, *Bull. Fac. Pharm. (Cairo Univ.)*, 2016, **54**(1), 77–86.
- 12 C. Zheng and S. L. You, *Chem. Soc. Rev.*, 2012, **41**, 2498–2518.
- 13 W. Chen, Z. Liu, J. Tian, J. Li, J. Ma, X. Cheng and G. Li, *J. Am. Chem. Soc.*, 2016, **138**, 12312–12315.
- 14 R. Lavilla, *J. Chem. Soc., Perkin Trans. 1*, 2002, **1**(1), 1141–1156.
- 15 A. Hantzs, *Justus Liebigs Ann. Chem.*, 1882, **215**, 1–82.
- 16 S. Palaniappan and A. John, *J. Mol. Catal. A: Chem.*, 2005, **233**, 9–15.
- 17 C. R. Reddy, B. Vijayakumar, P. Iyengar, G. Nagendrappa and B. J. Prakash, *J. Mol. Catal. A: Chem.*, 2004, **223**, 117–122.
- 18 K. Pajuste and A. Plotniece, *Chem. Heterocycl. Compd.*, 2016, **52**(8), 538–540.
- 19 B. Banerjee, *J. Nanostruct. Chem.*, 2017, **7**, 389–413.
- 20 V. Calvino-Casilda and R. M. Martín-Aranda, *Catal. Today*, 2020, **354**, 44–50.
- 21 J. C. Védrine, *Catalysts*, 2017, **7**, 341.
- 22 Z. L. Wang, *J. Mater. Sci. Eng.*, 2009, **64**, 33.
- 23 Z. Dehghanizadeh and F. Buazar, *J. Heterocycl. Chem.*, 2018, **8**(2), 18–25.
- 24 G. K. Reen, M. Ahuja, A. Kumar, R. Patidar and P. Sharma, *Org. Prep. Proced. Int.*, 2017, **49**(3), 273–286.
- 25 Y. M. Tao, S. Y. Ma, H. X. Chen, J. X. Meng, L. L. Hou, Y. F. Jia and X. R. Shang, *Vacuum*, 2011, **85**, 744.
- 26 Z. Zhang, J. B. Yi, J. Ding, L. M. Wong, H. L. Seng, S. J. Wang, J. G. Tao, G. P. Li, G. Z. Xing, T. C. Sum, C. H. A. Huan and T. Wu, *J. Phys. Chem. C*, 2008, **112**, 9579.
- 27 H. Alinezhad and S. M. Tavakkoli, *Res. Chem. Intermed.*, 2015, **41**, 5931–5940.
- 28 B. M. Sapkal, P. K. Labhane, S. T. Disale and D. H. More, *Lett. Org. Chem.*, 2019, **16**, 139–144.
- 29 S. D. Bajaj, P. V. Tekade, G. V. Lakhotiya and P. G. Borkar, *Acta Phys. Pol.*, 2017, **132**(4), 1294–1300.
- 30 B. B. F. Mirjalili, A. Bamoniri and L. A. Salmanpoor, *J. Nanostruct.*, 2018, **8**(3), 276–287.
- 31 K. K. Rao, D. T. Rao and B. N. Naidu, *Int. J. Res. Appl. Sci. Eng. Technol.*, 2017, **5**, 1913–1918.
- 32 A. Javidan, A. Ziarati and J. Safaei-Ghom, *Ultrason. Sonochem.*, 2014, **21**, 1150.
- 33 J. Safaei-Ghom, M. Kiani, A. Ziarati and H. Shahbazi-Alavi, *J. Sulfur Chem.*, 2014, **35**, 450.
- 34 J. Safaei-Ghom, H. Shahbazi-Alavi and R. Teymuri, *Polycycl. Aromat. Comp.*, 2016, 1–14.
- 35 S. V. H. S. Bhaskaruni, S. Maddila, W. E. V. Zyl and S. B. Jonnalagadda, *ACS Omega*, 2019, **4**, 21187–21196.
- 36 M. M. Heravi, T. Hosseinejad and N. Nazari, *Can. J. Chem.*, 2017, **95**(5), 530–536.
- 37 S. Tabassum, S. Govindaraju, R. R. Khan and M. A. Pasha, *RSC Adv.*, 2016, **6**, 29802–29810.
- 38 S. V. Ley, I. R. Baxendale, G. Brusotti, M. Caldarelli, A. Massi and M. Nesi, *Il Farmaco*, 2002, **57**(4), 321–330.
- 39 A. Rashidi, Z. Tavakoli, Y. Tarak, S. Khodabakhshi, M. K. Abbasabadi and M. J. Chin, *J. Am. Chem. Soc.*, 2016, **63**, 399.
- 40 A. K. Geim and K. S. Novoselov, *Nat. Mater.*, 2007, **6**, 183–191.
- 41 D. Fejes and K. Hernadi, *Materials*, 2010, **3**, 2618–2642.
- 42 J. N. Tiwari, R. N. Tiwari and K. S. Kim, *Prog. Mater. Sci.*, 2012, **57**(4), 724–803.
- 43 L. Moradi, R. Mahinpour, Z. Zahraei and N. Pahlevanzadeh, *J. Saudi Chem. Soc.*, 2018, **22**(7), 876–885.
- 44 L. Moradi and M. Zare, *Green Chem. Lett. Rev.*, 2018, **11**(3), 197–208.
- 45 T. Demirci, B. Celik, Y. Yıldız, S. Eriş, M. Arslan, F. Sen and B. Kilbas, *RSC Adv.*, 2016, **6**(80), 76948–76956.
- 46 M. Maheswara, V. Siddaiah, Y. K. Rao, Y. M. Tzeng and C. Sridhar, *J. Mol. Catal. A: Chem.*, 2006, **260**(1–2), 179–180.
- 47 T. W. Kim, R. Ryoo, K. P. Gierszal, M. Jaroniec, L. A. Solovyov, Y. Sakamoto and O. Terasaki, *J. Mater. Chem.*, 2005, **15**(15), 1560–1571.
- 48 M. Kruk, M. Jaroniec, R. Ryoo and J. M. Kim, *Chem. Mater.*, 1999, **11**(9), 2568–2572.
- 49 B. F. Mirjalili, A. Bamoniri and M. A. Mirhoseini, *Chem. Heterocycl. Compd.*, 2012, **48**, 856–860.
- 50 A. Bamoniri, B. B. F. Mirjalili and S. Fouladgar, *J. Taiwan Inst. Chem. Eng.*, 2016, **63**, 396–403.
- 51 F. Moheisenia, A. R. Kiasatc and R. Badria, *Polycycl. Aromat. Comp.*, 2019, 1–13.
- 52 R. Mirsafaei, S. Delzende and A. Abdolazimi, *Int. J. Environ. Sci. Technol.*, 2016, **13**(9), 2219–2226.
- 53 P. B. Thale, P. N. Borase and G. S. Shankarling, *RSC Adv.*, 2014, **4**(103), 59454–59461.
- 54 C. W. Lim and I. S. Lee, *Nano Today*, 2010, **5**(5), 412–434.
- 55 A. Maleki, M. Rabbani and S. Shahrokh, *Appl. Organomet. Chem.*, 2015, **29**(12), 809–814.



56 U. C. Rajesh, V. S. Pavan and D. S. Rawat, *RSC Adv.*, 2016, **6**(4), 2935–2943.

57 L. H. Reddy, J. L. Arias, J. Nicolas and P. Couvreur, *Chem. Rev.*, 2012, **112**, 5818.

58 A. R. Kiasat and J. Davarpanah, *J. Mol. Catal. A: Chem.*, 2013, **373**, 46–54.

59 B. Atashkar, A. Rostami and B. Tahmasbi, *Catal. Sci. Technol.*, 2013, **3**, 2140.

60 M. Gawande, A. Velhinho, I. Nogueira, C. A. A. Ghumman, O. M. N. D. Teodoro and P. Branco, *RSC Adv.*, 2012, **2**, 6144–6149.

61 A. R. Kiasat and S. Nazari, *J. Mol. Catal. A: Chem.*, 2012, **365**, 80–86.

62 L. A. Mercante, W. W. M. Melo, M. Granada, H. E. Troiani, W. A. A. Macedo, J. D. Ardison, M. G. F. Vaz and M. A. Novak, *J. Magn. Magn. Mater.*, 2012, **324**, 3029–3033.

63 N. S. Chaudhari, S. S. Warule, S. Muduli, B. B. Kale, S. Jouen, B. Lefez, B. Hannoyer and S. B. Ogale, *Dalton Trans.*, 2011, **40**, 8003.

64 F. B. Li, X. Z. Li, C. S. Liu and T. X. Liu, *J. Hazard. Mater.*, 2007, **149**, 199–207.

65 A. Maleki, R. Firouzi-Haji and Z. Hajizadeh, *Int. J. Biol. Macromol.*, 2018, **116**, 320–326.

66 A. Maleki, H. Movahed and P. Ravaghi, *Carbohydr. Polym.*, 2017, **156**, 259–267.

67 A. Maleki and M. Aghaei, *Ultrason. Sonochem.*, 2017, **38**, 585–589.

68 H. Li, P. S. Bhadury, B. Song and S. Yang, *RSC Adv.*, 2012, **2**(33), 12525–12551.

69 W. He, Z. Fang, K. Zhang, T. Tu, N. Lv, C. Qiu and K. Guo, *Chem. Eng. J.*, 2018, **331**, 161–168.

70 S. Igder, A. R. Kiasat and M. R. Shushizadeh, *Res. Chem. Intermed.*, 2015, **41**(10), 7227–7244.

71 R. Taheri-Ledari, J. Rahimi and A. Maleki, *Ultrason. Sonochem.*, 2019, **59**, 104737.

72 F. Heidarizadeh, *J. Magn. Magn. Mater.*, 2017, **428**, 481–487.

73 A. Bamoniri and S. Fouladgar, *RSC Adv.*, 2015, **5**(96), 78483–78490.

74 M. Ghanbari, S. Moradi and M. Setoodehkhah, *Green Chem. Lett. Rev.*, 2018, **11**(2), 111–124.

75 B. Maleki, A. V. Mofrad, R. Tayebee, A. Khojastehnezhad, H. Alinezhad and E. R. Seresht, *Russ. J. Gen. Chem.*, 2017, **87**(12), 2922–2929.

76 T. R. R. Naik and S. A. Shivashankar, *Tetrahedron Lett.*, 2016, **57**(36), 4046–4049.

77 Z. Hajizadeh, A. Maleki, J. Rahimi and R. Eivazzadeh-Keihan, *Silicon*, 2020, **12**, 1247–1256.

78 E. Pourian, S. Javanshir, Z. Dolatkhah, S. Molaei and A. Maleki, *ACS Omega*, 2018, **3**(5), 5012–5020.

79 A. Maleki, V. Eskandarpour, J. Rahimi and N. Hamidi, *Carbohydr. Polym.*, 2019, **208**, 251–260.

80 P. G. Mandhane, R. S. Joshi, D. R. Nagargoje and C. H. Gill, *Chin. Chem. Lett.*, 2011, **22**(5), 563–566.

81 R.-Y. Guo, Z.-M. An, L.-P. Mo, R.-Z. Wang, H.-X. Liu, S.-X. Wang and Z.-H. Zhang, *ACS Comb. Sci.*, 2013, **15**, 557–563.

82 R.-Y. Guo, Z.-M. An, L.-P. Mo, S.-T. Yang, H.-X. Liu, S.-X. Wang and Z.-H. Zhang, *Tetrahedron Lett.*, 2013, **69**(47), 9931–9938.

83 M. Chetia, A. A. Ali, D. Bhuyan, L. Saikia and D. Sarma, *New J. Chem.*, 2015, **39**(8), 5902–5907.

84 H. Hassani, B. Zakerinasab, M. A. Nasseri and M. Shavakandi, *RSC Adv.*, 2016, **6**(21), 17560–17566.

85 J.-H. Wang, G.-M. Tang, S.-C. Yan, Y.-T. Wang, S.-J. Zhan, E. Zhang, Y. Sun, Y. Jiang and Y.-Z. Cui, *Appl. Organomet. Chem.*, 2016, **30**(12), 1009–1021.

86 N. Ahmed and Z. N. Siddiqui, *ACS Sustain. Chem. Eng.*, 2015, **3**(8), 1701–1707.

87 B. Maleki, H. Atharifar, O. Reiser and R. Sabbaghzadeh, *Polycycl. Aromat. Comp.*, 2019, 1–14.

88 P. Wu, L. Feng, Y. Liang, X. Zhang, B. Mahmoudid and M. Kazemnejadi, *Appl. Catal., A*, 2020, **590**, 117301.

89 J. Safari, F. Azizi and M. Sadeghi, *New J. Chem.*, 2015, **39**(3), 1905–1909.

90 A. Maleki, M. Kamalzare and M. Aghaei, *J. Nanostruct. Chem.*, 2014, **5**(1), 95–105.

91 A. Maleki, R. Firouzi-Haji and Z. Hajizadeh, *Int. J. Biol. Macromol.*, 2018, **116**, 320–326.

92 K. Javanmiri and R. Karimian, *Monatsh. Chem.*, 2020, **151**, 199–212.

93 M. G. Dehbalaei, N. Foroughifar, A. Khajeh-Amiri and H. Pasdar, N-propylbenzoguanamine, *J. Chin. Chem. Soc.*, 2018, **65**(11), 1356–1369.

94 L. Z. Fekri, K. H. Pour and S. Zeinali, *J. Organomet. Chem.*, 2020, **915**, 121232.

95 T. Amoli and S. M. Baghbanian, *Res. Chem. Intermed.*, 2018, **44**, 3389–3405.

96 K. Valadi, S. Gharibi, R. Taheri-Ledari and A. Maleki, *Solid State Sci.*, 2020, **101**, 106141.

97 M. Khodamorady, S. Sohrabnezhad and K. Bahrami, *Polyhedron*, 2020, **178**, 114340.

98 A. Khaskel, P. Barman and U. Janab, *RSC Adv.*, 2015, **5**(18), 13366–13373.

